Tunable optofluidic aperture configured by a liquid-core/liquid-cladding structure

Chaolong Song,[1] Nam-Trung Nguyen,[1,*] Anand Krishna Asundi,[1] and Cassandra Lee-Ngo Low[2]

[1]*School of Mechanical and Aerospace Engineering, Nanyang Technological University, 50 Nanyang Avenue, Singapore 639798, Singapore*

[2]*School of Electrical and Electronic Engineering, Singapore Polytechnic, 500 Dover Road, Singapore 139651, Singapore*

**Corresponding author: mntnguyen@ntu.edu.sg*

Received March 23, 2011; revised April 5, 2011; accepted April 5, 2011;
posted April 6, 2011 (Doc. ID 144555); published May 5, 2011

Miniaturized and tunable optical components, such as the waveguide, lens, and prism, have been of great interest for lab-on-chip systems. This Letter reports an optofluidic aperture stop formed by the liquid-core/liquid-cladding flow. The aperture size can be tuned accordingly by adjusting the flow rates. Manipulation of the aperture size allows control of the amount of light passing through the corresponding optical system as well as the angular aperture on the image side. This optofluidic aperture enables lab-on-chip optical systems to have a greater flexibility and more functionalities. © 2011 Optical Society of America

OCIS codes: 230.3990, 230.4685, 050.1965, 080.3620.

Recent research has been intensively focused on the development of optofluidic components for the miniaturization of lab-on-chip systems [1]. Optical components configured by the flow of liquids such as waveguides [2], lenses [3], and prisms [4] have been realized in microfluidic networks. One motivation to integrate optical components into microfluidics is to miniaturize the whole system and to reduce the overall cost. Instead of using a bulky external optical system, optofluidic systems can be made compact and portable for field use [5]. Further more, the liquid/liquid interface can be deformed by shear stress, making optofluidic components dynamically tunable. Recent works have shown that the optical properties of the optofluidic components can be well predefined mathematically [6,7].

The aperture stop or entrance pupil is an important optical component in imaging and detection systems. This component determines the amount of light passing through the optical system as well as the angular aperture on the object side. Previous works have demonstrated tunable out-of-plane apertures using microfabrication technology [8–10]. The problem of these apertures is the difficulty to integrate them into microfluidics. Recently, a simple aperture in a microfluidic network built by filling ink into a microchannel was reported [11]. But the size of this aperture remains fixed after fabrication. This Letter proposes and demonstrates a tunable optofluidic aperture stop, which can be dynamically reconfigured according to the flow condition.

The schematic configuration of the optofluidic aperture is illustrated in Fig. 1(a). A liquid-core/liquid-cladding structure was used to form this aperture. The core liquid is optically transparent, allowing light rays to pass through, while the ink with negligible optical transmittance (≈0%) works as the cladding liquid, blocking the propagation of light. To test the optical performance of the aperture, an optical fiber inserted in an alignment groove mimics an axial point light source; an optofluidic lens is positioned after the aperture to represent a lens system. A ray-tracing chamber filled with fluorescent liquid is placed on the image side to visualize the light rays, which have gone through the aperture as well as the lens. When the aperture is tuned with a given flow rate ratio ($\phi = Q_{\text{cladding}}/Q_{\text{core}}$), the mount of the light that reaches the image space as well as the angular aperture on the image side can be adjusted accordingly.

To test this concept, the device was fabricated by molding poly dimethylsiloxane (PDMS) on a master made of a thick resist called SU-8 [12]. The channel depth was defined to be 150 μm by choosing a proper spin coating speed for the SU-8. The distance between the fiber tip and the center of aperture is 3 mm. The lens is positioned 1 mm away from the aperture. The dimension of the rectangular chamber for forming the optofluidic aperture is 1 mm × 0.6 mm, and the diameter of the circular chamber for the optofluidic lens is 1 mm. Figure 1(b) shows a typical situation in which a point light source is projected to the image space by the lens with its light cone restricted by the optofluidic aperture. The core liquid of the aperture is a mixture (viscosity $\mu = 9 \times 10^{-3}$ Pa s at 25 °C) of glycerol (60% by weight) and water (40% by weight) with a refractive index of $n = 1.412$ matching

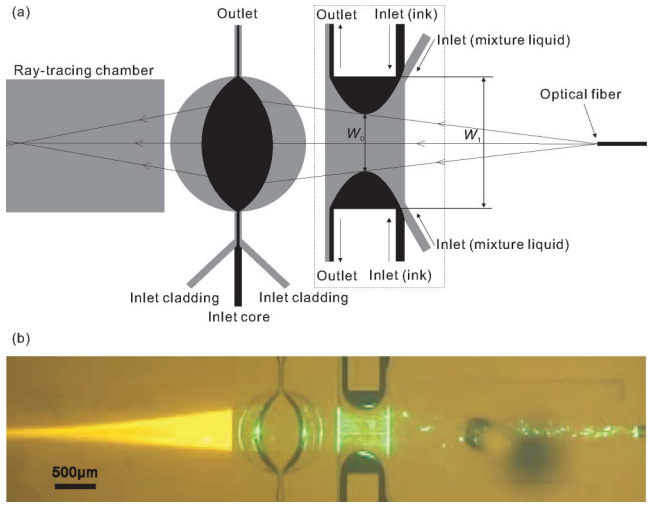

Fig. 1. (Color online) Illustration of the optical system to test the performance of the optofluidic aperture. For the test, the focal length of the optofluidic lens is fixed, while the flow rate ratio of the optofluidic aperture is adjusted to control the radiant flux and angular aperture of the light beam. (a) Schematic configuration and (b) bright field image.

 © 2011 Optical Society of America

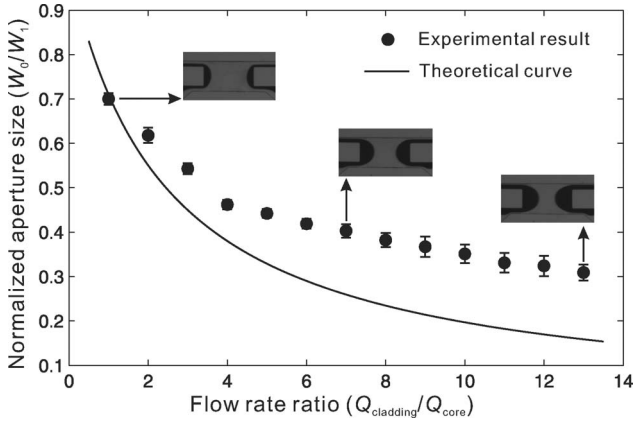

Fig. 2. Relationship between the aperture size (normalized by 1 mm) and the flow rate ratio. The flow rate of the core stream (transparent liquid) is fixed at 200 μl/h, while the flow rate of the cladding stream (black ink) is variable from 200 to 2600 μl/h.

that of the PDMS. The light-blocking cladding is black ink (viscosity $\mu = 2.0 \times 10^{-3}$ Ns/m^2 at 25 °C). The core and cladding liquids of the optofluidic lens are cinnamaldehyde (viscosity $\mu = 5.7 \times 10^{-3}$ Ns/m^2 at 25 °C and refractive index $n = 1.62$) and a mixture of 73.5% ethylene glycol and 26.5% ethanol (viscosity $\mu = 9.8 \times 10^{-3}$ Ns/m^2 at 25 °C and refractive index $n = 1.412$), respectively.

The relationship between the aperture size and the flow rate ratio ($\phi = Q_{\text{cladding}}/Q_{\text{core}}$) was first investigated. The flow can dynamically change the aperture size using the phenomenon of hydrodynamic spreading [13]:

$$W_0/W_1 = 1/(2\beta\phi + 1), \tag{1}$$

where W_0 and W_1 are the widths of the core stream and the channel, respectively (Fig. 1). β and ϕ are the viscosity ratio and the flow rate ratio between the cladding and core streams, respectively. The low aspect ratio of 0.6 between the chamber length and width leads to curved streamlines, which cause the discrepancy between the experimental results and the theoretical prediction for a ratio of infinity; see Fig. 2.

In the test, the flow rate of the core stream (mixture of glycerol and water) was fixed at 200 μl/h. The flow rate of the cladding stream (black ink) was varied from 200 to 2600 μl/h. Owing to the low Reynolds number, the flow inside the rectangular chamber is laminar. The streamlines are smooth, and the fluid motion is steady. Consequently, the aperture size is set once the flow condition is fixed. According to the theory of hydrodynamic spreading, the width of the ink flow (cladding stream) was narrower than that of the transparent flow (core stream) at a low flow rate ratio. Thus, an aperture with a large diameter can be realized. When the flow rate ratio was increased, the cladding stream squeezed the core stream to be narrower, leading to a smaller aperture. Figure 2 shows the experimental results of the flow rate ratio dependence changing the aperture size from 700 to 309 μm. The insets of Fig. 2 depict the optofluidic apertures at flow rate ratios of 1, 7, and 13, respectively. Although not shown here, if a large flow rate ratio is applied, this optofluidic aperture can be adjusted to have a very small size, which is only limited by the diffusion distance between fluids of about 60 μm under the flow condition reported in this Letter.

To assess the optical performance of this aperture, fluorescence dye Rhodamine B (Sigma Aldrich, excitation wavelength of 540 nm, emission wavelength of 625 nm) was diluted in a mixture of glycerol (60% by weight) and water (40% by weight) was injected into the ray-tracing chamber to visualize the light rays coming out from the aperture and the optofluidic lens. The flow rate ratio ($\phi = Q_{\text{cladding}}/Q_{\text{core}}$) for the lens was fixed at 6. A multimode optical fiber (AFS105/125Y, Thorlabs, Inc.) with an NA of 0.22 was inserted into a prefabricated microchannel with a width of 130 μm to mimic a point light source. The optical fiber introduced the light generated from a green laser with a wavelength of $\lambda = 532$ nm. When the light rays were incident on the rectangular chamber where the aperture was developed, the light cone was partially blocked while the paraxial part was allowed to pass through and be focused by the optofluidic lens. The light rays that finally reached the image space were visualized and recorded by a CCD camera. Figure 3 shows the light rays on the image side restricted by the apertures formed by flow rate ratios of 1, 7, and 13, respectively. A qualitative inspection of the ray-tracing results shows that the amount of light rays and the angular aperture on the image can be tuned by the flow rate ratio.

Furthermore, we quantitatively investigate how the optofluidic aperture controls the amount of light by regarding light as the flow of luminous energy along the geometric rays. Although the quantum yields of Rhodamine B are different for individual solutions, the amount of photons emitted can be considered to be proportional to the amount of photons absorbed by Rhodamine B in a specific solution [14]. The intensity of each pixel in the ray-tracing images can represent the local energy flux that the passing light ray carries. The fluorescence intensity value was integrated over the dotted line shown in Fig. 3, and we considered it as the radiant flux (the amount of light) through the optofluidic system consisting of the aperture and the lens. Figure 4(a) shows the experimental result of the radiant flux as a function of

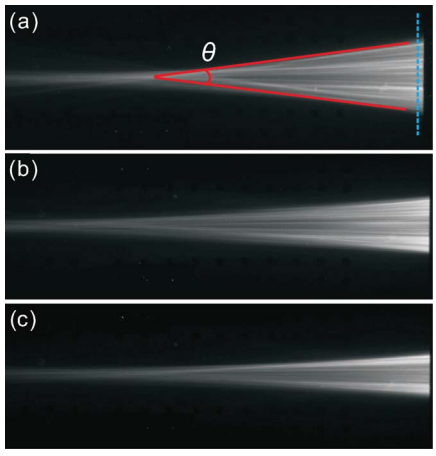

Fig. 3. (Color online) Light beam on the image side visualized by the fluorescence dye Rhodamine B can be dynamically controlled by tuning the optofluidic aperture size: flow rate ratio of (a) 1, (b) 7, and (c) 13.

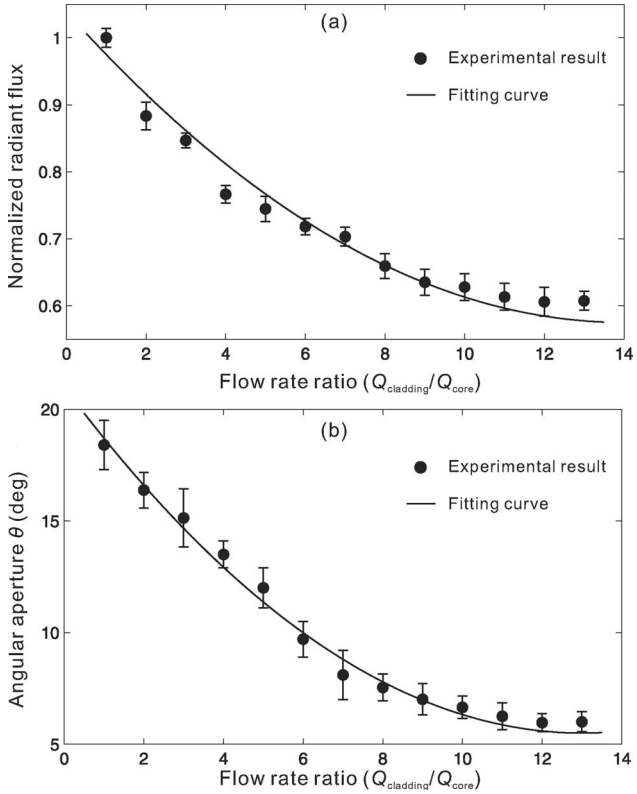

Fig. 4. (a) Radiant flux through the optical system as a function of the flow rate ratio. (b) The angular aperture on the image side as a function of the flow rate ratio.

the flow rate ratio. Increasing the flow rate ratio between the cladding and core stream squeezes the transparent liquid, resulting in a smaller aperture size and therefore causing less radiant flux to reach the image side. Previous research reported the integration of a lens into the microfluidic network to enhance the excitation of light for biochemical applications [5,15]. The proposed optofluidic aperture may be combined with this lens system to generate a more flexible and robust optical system to control the amount of light. Another interesting usage of this device is to control the angular aperture on the object side as well as the image side. By confining the light cone within the paraxial region with a small angular aperture, the spherical aberrations can be reduced significantly. Figure 4(b) shows the quantitative result of the angular aperture on the image side as a function of the flow rate ratio.

In conclusion, this Letter reports the design and demonstration of an optofluidic aperture stop. The device can be easily integrated into microfluidic networks and combined with previously proposed optofluidic components. The tunable aperture stop was realized by adjusting the flow rate ratio between an opaque cladding and a transparent core. The test results showed that the radiant flux through the optical system as well as the angular aperture on the image side can be precisely controlled by changing the flow rate ratio between the cladding and core.

References

1. V. R. Horowitz, D. D. Awschalom, and S. Pennathur, Lab Chip **8**, 1856 (2008).
2. D. B. Wolfe, R. S. Conroy, P. Garstecki, B. T. Mayers, M. A. Fischbach, K. E. Paul, M. Prentiss, and G. M. Whitesides, Proc. Natl. Acad. Sci. USA **101**, 12434 (2004).
3. X. Mao, J. R. Waldeisen, B. K. Juluri, and T. J. Huang, Lab Chip **7**, 1303 (2007).
4. C. Song, N. T. Nguyen, A. K. Asundi, and S. H. Tan, Opt. Lett. **35**, 327 (2010).
5. H. Y. Tan, W. K. Loke, Y. T. Tan, and N. T. Nguyen, Lab Chip **8**, 885 (2008).
6. C. Song, N. T. Nguyen, S. H. Tan, and A. K. Asundi, Lab Chip **9**, 1178 (2009).
7. C. Song, N. T. Nguyen, S. H. Tan, and A. K. Asundi, Microfluid. Nanofluid. **9**, 889 (2010).
8. H. Yu, G. Zhou, F. S. Chau, and F. Lee, Opt. Lett. **33**, 548 (2008).
9. C. G. Tsai and J. A. Yeh, Opt. Lett. **35**, 2484 (2010).
10. P. Müller, N. Spengler, H. Zappe, and W. Mönch, J. Microelectromech. Syst. **19**, 1477 (2010).
11. S. K. Y. Tang, C. A. Stan, and G. M. Whitesides, Lab Chip **8**, 395 (2008).
12. P. Abgrall, V. Conedera, F. Camon, A. M. Gue, and N. T. Nguyen, Electrophoresis **28**, 4539 (2007).
13. Z. Wu and N. T. Nguyen, Sens. Actuators B **107**, 965 (2005).
14. R. F. Kubin and A. N. Fletcher, J. Lumin. **27**, 455 (1982).
15. S. Camou, H. Fujita, and T. Fujii, Lab Chip **3**, 40 (2003).